We are IntechOpen, the world's leading publisher of Open Access books Built by scientists, for scientists

4,800
Open access books available

122,000
International authors and editors

135M
Downloads

Our authors are among the

154
Countries delivered to

TOP 1%
most cited scientists

12.2%
Contributors from top 500 universities

CLARIVATE ANALYTICS BOOK CITATION INDEX INDEXED

WEB OF SCIENCE™

Selection of our books indexed in the Book Citation Index in Web of Science™ Core Collection (BKCI)

Interested in publishing with us?
Contact book.department@intechopen.com

Numbers displayed above are based on latest data collected.
For more information visit www.intechopen.com

13

6-DOF Motion Sensor System Using Multiple Linear Accelerometers

Ryoji Onodera and Nobuharu Mimura
Tsuruoka National College of Technology, Niigata University
Japan

1. Introduction

This chapter describes a multi degrees of freedom (hereafter, "DOF") motion sensor system in 3D space. There are two major areas where multiple-DOF motion sensors are needed. The first involves vehicles, helicopters or humanoid robots, which are multi-input multi-output objects, each having 3 DOF in all translational and rotational directions. Thus, an accurate measurement of all 6 DOF motions is needed for their analysis and control. The second area involves considering not only the translational components, but also the rotational components for 1-DOF linear motion on ground since this type of motion is always affected to a certain extent by motion along other axes, and mixed signals of translational and rotational components are detected in the case of using 1-DOF motion sensors.

So far, inertial navigation systems (INS) with highly accurate gyro sensors and accelerometers have been used in the field of rocketry and aerodynamics. However, it is difficult to install such systems combined with gyroscopes and accelerometers on small robots due to their large size, weight and cost. In recent years, small vibration gyro systems and micro-machine gyro systems have been developed by using MEMS (micro-electro-mechanical system) technology. However, the sensor units which utilize these systems are not small, weighing about 6 to 10 kilograms, and in addition there are some problems with measurement accuracy and stability.

In the case of multiaxial sensors, it is known that the specific problem of non-linear cross effect arises, which means that other axial components interfere with the target one, and the measured values differ from the true values due to this effect. As a result, the cross effect reduces the measurement accuracy. In addition, as a result of increasing the effect by the gain and offset errors of each axis, stability is lost. Therefore, sensor calibration is required for suppressing the cross effect, as well as for decreasing the gain and offset errors. However, in general, gyro systems cannot be calibrated in isolation, which needs special equipments, such as an accurate rotary table, for generating a nominal motion. Thus, a proper calibration of the multiaxial sensors by the user is extremely difficult.

In the present work, we propose a newly developed 6-DOF motion sensor using only multiple accelerometers, without the gyro system. The advantage of using accelerometers is that they can be calibrated with relative ease, using only the gravitational acceleration without any special equipment. So far, we have performed several experiments using the

prototype sensor, and observed rapid divergence followed by the specific cross effect in the multiaxial sensors. Therefore, in this chapter, we investigate these two problems of divergence and cross effect. Regarding the divergence, we analyzed the stability based on the geometric structure of the sensor system. Furthermore, we analyzed the cross effect with respect to the alignment error of the linear accelerometer, and proposed a relatively easy calibration method based on the analytical results. Finally, we investigated the proposed system and methods in an experiment involving vehicle motion, which is particularly prone to the cross effect, and demonstrated that this sensor system (i.e., the 6-DOF accelerometer) performs well.

2. Measurement principle and extension to multiple axes

First, we consider the acceleration which occurs at point *i* on a rigid body (Fig.1). We define a position vector for the moving origin of the body (Σ_b) relative to the reference frame (Σ_o) as ${}^o\boldsymbol{p}_b = [{}^o p_{bx} \quad {}^o p_{by} \quad {}^o p_{bz}]^T$, and the position vector of the point *i* relative to the body origin as ${}^o\boldsymbol{r}_i = [{}^o r_{ix} \quad {}^o r_{iy} \quad {}^o r_{iz}]^T$. Then, the position vector ${}^o\boldsymbol{p}_b$ from Σ_o is is represented as follows:

$$ {}^o\boldsymbol{p}_i = {}^o\boldsymbol{p}_b + {}^o\boldsymbol{r}_i . \tag{1} $$

When the rigid body revolves around the origin Σ_b , Eq.(1) is written as

$$ {}^o\dot{\boldsymbol{p}}_i = {}^o\dot{\boldsymbol{p}}_b + {}^o\dot{\boldsymbol{\omega}}_b \times {}^o\boldsymbol{r}_i . \tag{2} $$

Moreover, we can rewrite the equation by taking into consideration the gravitational acceleration as follows:

$$ {}^o\ddot{\boldsymbol{p}}_i = {}^o\ddot{\boldsymbol{p}}_b + \boldsymbol{g} + {}^o\dot{\boldsymbol{\omega}}_b \times {}^o\boldsymbol{r}_i + {}^o\boldsymbol{\omega}_b \times \left({}^o\boldsymbol{\omega}_b \times {}^o\boldsymbol{r}_i \right). \tag{3} $$

Equation (3) represents the acceleration of point *i* on the body. If one linear accelerometer is installed at point *i*, the accelerometer output a_i is

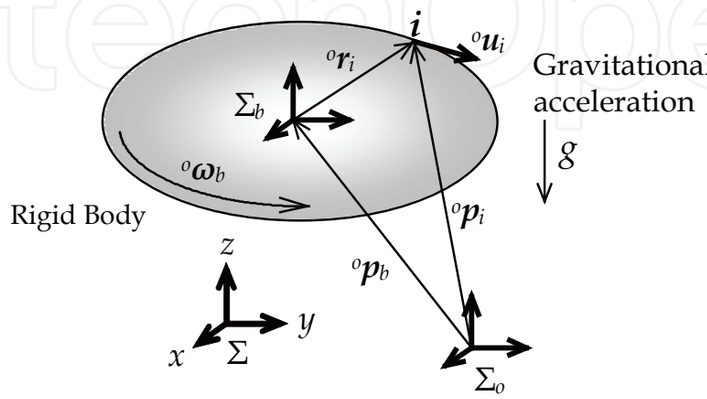

Fig. 1. Acceleration at point *i* on a rigid body

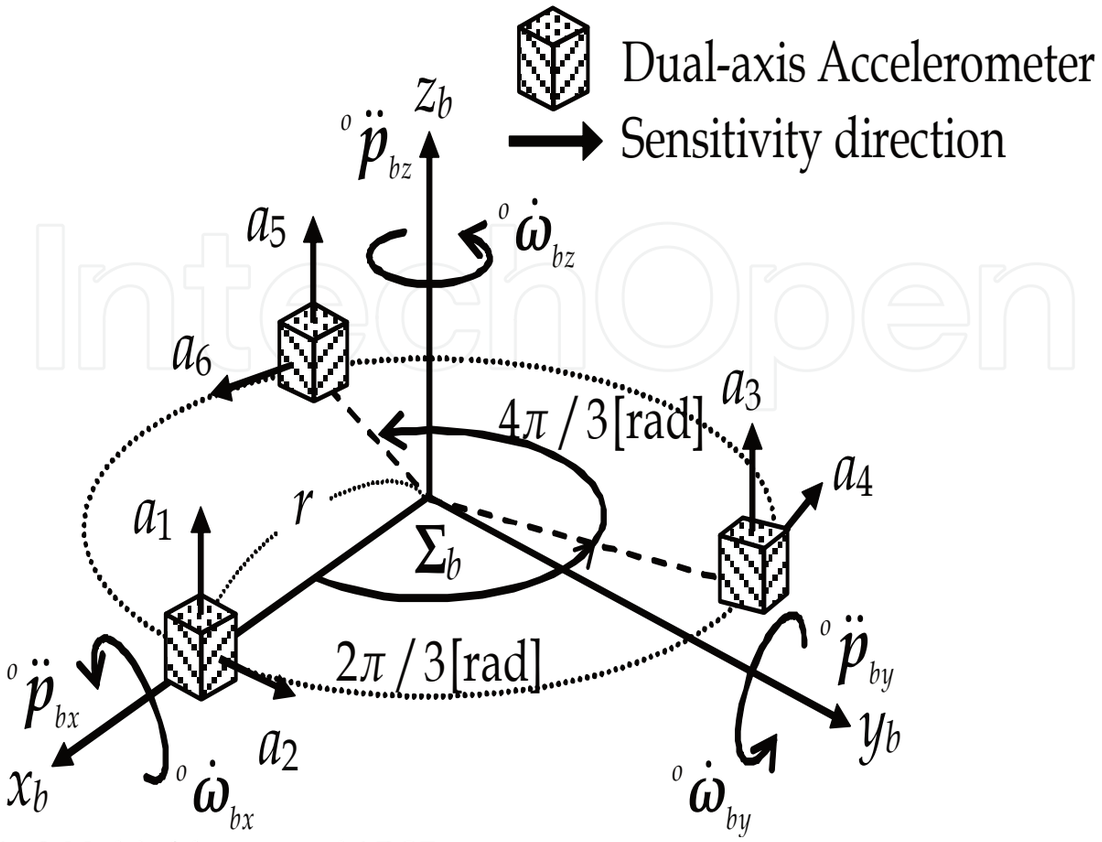

Fig. 2. Model of the proposed 6-DOF measurement system

$$\begin{aligned} a_i &= {}^o\boldsymbol{u}_i^T\,{}^o\ddot{\boldsymbol{p}}_i \\ &= \begin{bmatrix} {}^o\boldsymbol{u}_i^T & {}^o\boldsymbol{u}_i^T\,{}^o\boldsymbol{R}_i \end{bmatrix} \begin{bmatrix} {}^o\ddot{\boldsymbol{p}}_b + \boldsymbol{g} \\ {}^o\dot{\boldsymbol{\omega}}_b \end{bmatrix} + {}^o\boldsymbol{u}_i^T \left\{ {}^o\boldsymbol{\omega}_b \times \left({}^o\boldsymbol{\omega}_b \times {}^o\boldsymbol{r}_i \right) \right\}, \end{aligned} \tag{4}$$

where

$${}^o\boldsymbol{R}_i = \begin{bmatrix} 0 & -{}^or_{iz} & {}^or_{iy} \\ {}^or_{iz} & 0 & -{}^or_{ix} \\ -{}^or_{iy} & {}^or_{ix} & 0 \end{bmatrix}. \tag{5}$$

Here, ${}^o\boldsymbol{u}_i = [{}^ou_{ix} \quad {}^ou_{iy} \quad {}^ou_{iz}]^T$ is the sensitivity unit vector. In Eq.(3), the translational, rotational, centrifugal and gravitational accelerations are mixed, and cannot be separated using only one accelerometer output. In order to obtain 6-DOF acceleration data (i.e., data regarding translational and rotational motion), we need to resolve multiple acceleration signals, when more than six linear accelerometers are needed. Thus, in the six accelerometers, each output is given by (see Fig.2)

$$\begin{bmatrix} a_1 \\ a_2 \\ \vdots \\ a_6 \end{bmatrix} = {}^{o}\boldsymbol{R} \begin{bmatrix} {}^{o}\ddot{\boldsymbol{p}}_b + \boldsymbol{g} \\ {}^{o}\dot{\boldsymbol{\omega}}_b \end{bmatrix} + \begin{bmatrix} {}^{o}\boldsymbol{u}_1{}^{T}\left\{ {}^{o}\boldsymbol{\omega}_b \times \left({}^{o}\boldsymbol{\omega}_b \times {}^{o}\boldsymbol{r}_1 \right) \right\} \\ {}^{o}\boldsymbol{u}_2{}^{T}\left\{ {}^{o}\boldsymbol{\omega}_b \times \left({}^{o}\boldsymbol{\omega}_b \times {}^{o}\boldsymbol{r}_2 \right) \right\} \\ \vdots \\ {}^{o}\boldsymbol{u}_6{}^{T}\left\{ {}^{o}\boldsymbol{\omega}_b \times \left({}^{o}\boldsymbol{\omega}_b \times {}^{o}\boldsymbol{r}_6 \right) \right\} \end{bmatrix}, \tag{6}$$

where

$$ {}^{o}\boldsymbol{R} = \begin{bmatrix} {}^{o}\boldsymbol{u}_1{}^{T} & -{}^{o}\boldsymbol{u}_1{}^{T}{}^{o}\boldsymbol{R}_1 \\ {}^{o}\boldsymbol{u}_2{}^{T} & -{}^{o}\boldsymbol{u}_2{}^{T}{}^{o}\boldsymbol{R}_2 \\ \vdots & \vdots \\ {}^{o}\boldsymbol{u}_6{}^{T} & -{}^{o}\boldsymbol{u}_6{}^{T}{}^{o}\boldsymbol{R}_6 \end{bmatrix}. \tag{7}$$

${}^{o}\boldsymbol{R}$ is a gain matrix which depends on the direction of the sensitivity vectors and position vectors. ${}^{o}\boldsymbol{R}$ is a known constant matrix. If ${}^{o}\boldsymbol{R}$ is a non-singular matrix, Eq.(6) can be written as

$$\begin{bmatrix} {}^{o}\ddot{\boldsymbol{p}}_b + \boldsymbol{g} \\ {}^{o}\dot{\boldsymbol{\omega}}_b \end{bmatrix} = {}^{o}\boldsymbol{R}^{-1} \begin{bmatrix} a_1 \\ a_2 \\ a_3 \\ a_4 \\ a_5 \\ a_6 \end{bmatrix} - \begin{bmatrix} -0.03\left({}^{o}\omega_{bx}{}^{2} - {}^{o}\omega_{by}{}^{2} \right) \\ 0.06\,{}^{o}\omega_{bx}\,{}^{o}\omega_{by} \\ 0 \\ {}^{o}\omega_{by}\,{}^{o}\omega_{bz} \\ -{}^{o}\omega_{bx}\,{}^{o}\omega_{bz} \\ 0 \end{bmatrix}, \tag{8}$$

where

$$\left[{}^{o}\ddot{\boldsymbol{p}}_b + \boldsymbol{g} \right] = \begin{bmatrix} {}^{o}\ddot{p}_{bx} - g\,{}^{o}\theta_{by} \\ {}^{o}\ddot{p}_{by} + g\,{}^{o}\theta_{bx} \\ {}^{o}\ddot{p}_{bz} + g \end{bmatrix}, \left[{}^{o}\dot{\boldsymbol{\omega}}_b \right] = \begin{bmatrix} {}^{o}\dot{\omega}_{bx} \\ {}^{o}\dot{\omega}_{by} \\ {}^{o}\dot{\omega}_{bz} \end{bmatrix}. \tag{9}$$

Here, the terms consisting of angular velocities $({}^{o}\omega_{bx}, {}^{o}\omega_{by}, {}^{o}\omega_{bz})$ are the centrifugal acceleration components in Eq.(8). We tentatively refer to these terms as "CF terms". Furthermore, ${}^{o}\theta_{bx}$ and ${}^{o}\theta_{by}$ are the attitude angle of the *x* axis (roll) and the *y* axis (pitch), respectively. In addition, the distance *r* between Σ_b and each accelerometer is 0.06 m.

3. Stability analysis

In motion sensor systems, one of the most serious problems is the drift effect. Although it occurs for various reasons (e.g., vibration or environmental temperature fluctuations), if the solutions are obtained only from the accelerometer outputs (that is, if they are represented by an algebraic equation), they can be improved with relatively high accuracy by performing sensor calibration. However, as shown in Eq.(8) of this system, the z axis acceleration is resolved only by accelerometer outputs (a_1-a_6), while the x and y axis accelerations are resolved by outputs and CF terms with the cross effect in each other. In past studies, it has been indicated that these terms interact with each other, starting with the drift error. As a result, a rapid divergence of the solutions (i.e., the 6-DOF acceleration) caused by the cross effect in addition to the drift error has already been confirmed in past systems. Therefore, in order to analyze the stability of the proposed system in the same case, let us assume the measurement errors occurring as follows:

$$\begin{aligned} {}^{o}\dot{\boldsymbol{\omega}}_b &= {}^{o}\dot{\boldsymbol{\omega}}_{bn} + \Delta^{o}\dot{\boldsymbol{\omega}}_b, \\ a_i &= a_{in} + \Delta a_i \quad (i = 1,2,...,6), \end{aligned} \tag{10}$$

where the suffix n represents a true value, and Δ represents the combined error with gain and offset error. Here, we substitute Eq.(10) into Eq.(8) and solve the equation for the error terms (Δ). As a result, we obtain the following second-order differential equations for the error:

$$\begin{cases} \Delta^{o}\ddot{\omega}_{bx}(n) - \dfrac{{}^{o}\dot{\omega}_{bzn}(n)}{{}^{o}\omega_{bzn}(n)}\Delta^{o}\dot{\omega}_{bx}(n) + {}^{o}\omega_{bzn}{}^{2}(n)\Delta^{o}\omega_{bx}(n) = F_x(\Delta a_i(n)) \\ \Delta^{o}\ddot{\omega}_{by}(n) - \dfrac{{}^{o}\dot{\omega}_{bzn}(n)}{{}^{o}\omega_{bzn}(n)}\Delta^{o}\dot{\omega}_{by}(n) + {}^{o}\omega_{bzn}{}^{2}(n)\Delta^{o}\omega_{by}(n) = F_y(\Delta a_i(n)) \end{cases}, \tag{11}$$

where we assume that the above errors are negligibly small, and thus we obtain Eq.(11) by linear approximation.

$$\begin{aligned} &\Delta^{o}\boldsymbol{\omega}_b(n) << 0, \\ &\Delta^{o}\boldsymbol{\omega}_b(n)\cdot\Delta^{o}\boldsymbol{\omega}_b(n) \approx 0. \end{aligned} \tag{12}$$

Equation (11) is a Mathew-type differential equation, which is known to be intrinsically unstable, and therefore we analyzed Eq.(11) by using numerical calculation in order to clarify the stability or instability conditions of the 6-DOF sensor system.

The analytical result is shown in Fig.3, which shows the state of the amplitudes of the error terms ($\Delta^{o}\boldsymbol{\omega}_b$) for the frequency ratio $\omega_{x\,\mathrm{or}\,y}/\omega_z\,(\omega = 2\pi f)$ when time approached infinity. Here, ω_x, ω_y and ω_z represent the roll, pitch, and yaw frequencies, respectively. This result shows the error terms increase rapidly when the frequency ratio becomes even (i.e., $\omega_{x\,\mathrm{or}\,y}/\omega_z = 2.0, 4.0\,\mathrm{or}\,6.0\ldots$).

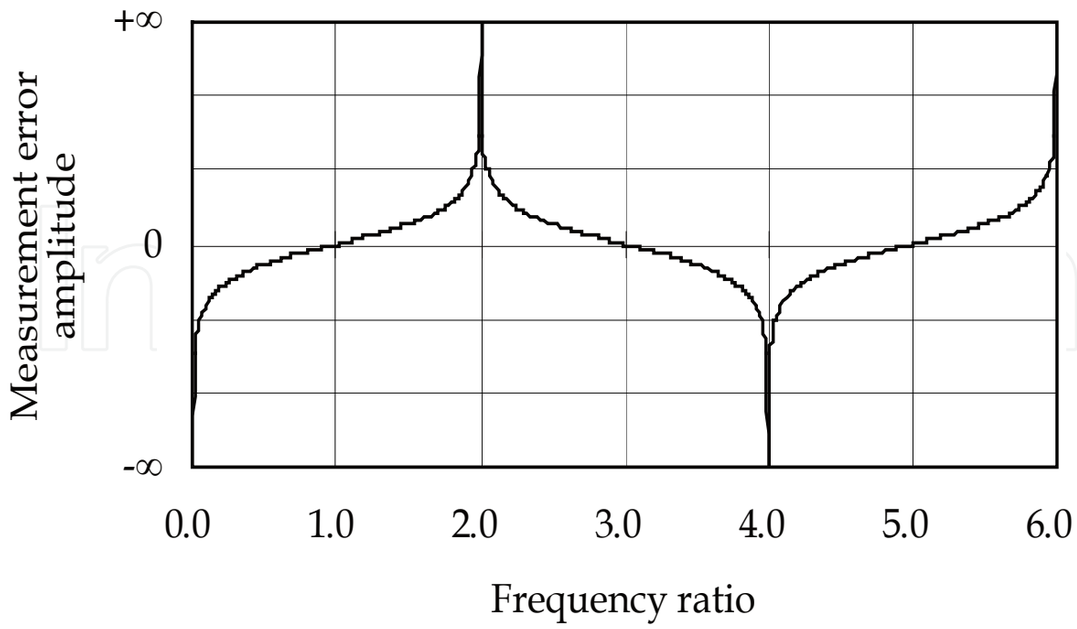

Fig. 3. Measurement error amplitude as plotted against the frequency ratio

Thus, it is considered that this system might become unstable when the roll or the pitch frequency become even for the yaw motion. However, in 3D motion of a rigid body, it is unlikely that the rigid body motion satisfies the above instability condition since the roll or pitch motion is generally synchronized with the yaw motion. This condition is likely to occur in specific cases, such as machinery vibration. Thus, conversely, it is unlikely that the system becomes unstable as a result of the above condition in a rigid body motion, such as the motion of a vehicle or an aircraft. However, the rapid divergence seen in Fig.3 is likely to occur when the system satisfies this condition due to measurement errors or the cross effect induced by the alignment error in this system. In the next section, we analyze the estimated alignment error and investigate a sensor calibration in order to minimize it.

4. Sensor calibration

4.1 Accelerometer error analysis

This sensor system obtains 6 DOF accelerations by resolving multiple linear acceleration signals. Therefore, the sensitivity vector ($^{o}\boldsymbol{u}_i$) and the position vector ($^{o}\boldsymbol{r}_i$) of the linear accelerometers must be exact. In the previous section, we investigated the case for each accelerometer without considering the alignment errors. Therefore, in this section, we investigate the accelerometer outputs a_{mi} by taking into account the error terms $\Delta^{o}\boldsymbol{u}_i$ and $\Delta^{o}\boldsymbol{r}_i$, which constitute the alignment errors of this sensor. Additionally, since accelerometers generally have offset errors, we assume the offset error to be Δa_{ofi}, in which case the accelerometer outputs with these alignment errors can be written as follows:

$$\begin{aligned}
\boldsymbol{a}_m &= \left({}^o\boldsymbol{R}+\Delta^o\boldsymbol{R}\right)\begin{bmatrix} {}^o\ddot{\boldsymbol{p}}_b+\boldsymbol{g} \\ {}^o\dot{\boldsymbol{\omega}}_b \end{bmatrix} + \begin{bmatrix} \left({}^o\boldsymbol{u}_i^{\,T}+\Delta^o\boldsymbol{u}_i^{\,T}\right)\left[{}^o\boldsymbol{\omega}_b\times\left\{{}^o\boldsymbol{\omega}_b\times\left({}^o\boldsymbol{r}_i^{\,T}+\Delta^o\boldsymbol{r}_i^{\,T}\right)\right\}\right] \end{bmatrix} + \Delta\boldsymbol{a}_{of} \\
&= \left({}^o\boldsymbol{R}+\Delta^o\boldsymbol{R}\right)\begin{bmatrix} {}^o\ddot{\boldsymbol{p}}_b+\boldsymbol{g} \\ {}^o\dot{\boldsymbol{\omega}}_b \end{bmatrix} + \left(\boldsymbol{c}_{rvi}+\Delta\boldsymbol{c}_{rvi}\right)vec\left({}^o\boldsymbol{\Omega}_b^{\,T}\right)+\Delta\boldsymbol{a}_{of}, \qquad (13) \\
\boldsymbol{a}_m &= \begin{bmatrix} a_{m1} & a_{m2} & \cdots & a_{m6} \end{bmatrix}^T, \\
\Delta\boldsymbol{a}_{of} &= \begin{bmatrix} \Delta a_{of1} & \Delta a_{of2} & \cdots & \Delta a_{of6} \end{bmatrix}^T,
\end{aligned}$$

where

$$\begin{aligned}
\left({}^o\boldsymbol{R}+\Delta^o\boldsymbol{R}\right) &= \left[{}^o\boldsymbol{u}_i^{\,T}+\Delta^o\boldsymbol{u}_i^{\,T} \quad -\left({}^o\boldsymbol{u}_i^{\,T}+\Delta^o\boldsymbol{u}_i^{\,T}\right)\left({}^o\boldsymbol{R}_i+\Delta^o\boldsymbol{R}_i\right)\right], \\
\left(\boldsymbol{c}_{rvi}+\Delta\boldsymbol{c}_{rvi}\right) &= \left[vec\left\{\left({}^o\boldsymbol{u}_i\,{}^o\boldsymbol{r}_i^{\,T}\right)\right\}^T\right]+\left[vec\left\{\left(\Delta^o\boldsymbol{u}_i\,{}^o\boldsymbol{r}_i^{\,T}\right)\right\}^T\right]+\left[vec\left\{\left({}^o\boldsymbol{u}_i\Delta^o\boldsymbol{r}_i^{\,T}\right)\right\}^T\right]+\left[vec\left\{\left(\Delta^o\boldsymbol{u}_i\Delta^o\boldsymbol{r}_i^{\,T}\right)\right\}^T\right],
\end{aligned}$$

$$vec\left(\begin{bmatrix} a_{11} & a_{12} & a_{13} \\ a_{21} & a_{22} & a_{23} \\ a_{31} & a_{32} & a_{33} \end{bmatrix}\right) = \begin{bmatrix} a_{11} & a_{21} & a_{31} & a_{12} & a_{22} & a_{32} & a_{13} & a_{23} & a_{33} \end{bmatrix}^T, \qquad (14)$$

$${}^o\boldsymbol{\Omega}_b = \left({}^o\boldsymbol{\omega}_b\times{}^o\boldsymbol{\omega}_b\times\right) = \begin{bmatrix} -\left({}^o\omega_{by}{}^2+{}^o\omega_{bz}{}^2\right) & {}^o\omega_{bx}\,{}^o\omega_{by} & {}^o\omega_{bx}\,{}^o\omega_{bz} \\ {}^o\omega_{bx}\,{}^o\omega_{by} & -\left({}^o\omega_{bx}{}^2+{}^o\omega_{bz}{}^2\right) & {}^o\omega_{by}\,{}^o\omega_{bz} \\ {}^o\omega_{bx}\,{}^o\omega_{bz} & {}^o\omega_{by}\,{}^o\omega_{bz} & -\left({}^o\omega_{bx}{}^2+{}^o\omega_{by}{}^2\right) \end{bmatrix}.$$

In Eqs.(13) and (14), Δa_{ofi} and $\Delta^o\boldsymbol{u}_i$ are based on Table 1, and $\Delta^o\boldsymbol{r}_i$ is based on the accuracy of the finish for the base frame. The sensor frame was cut by NC machinery. Its machining accuracy is ± 0.1 [mm] and ± 0.1 [deg] or better in a length accuracy and an angular accuracy, respectively. The results of calculating the maximum range of each term are shown in Table 2 when the above performance and accuracy are considered. As a result, the terms including $\Delta^o\boldsymbol{r}_i$ can be omitted since they are negligibly small in comparison to the other terms, as seen clearly from Table 2. Thus, we should consider only accelerometer errors including $\Delta^o\boldsymbol{u}_i$, and the error terms (i.e., $\Delta^o\boldsymbol{R}$ and $\Delta\boldsymbol{c}_{rvi}$) can be written as follows;

$$\Delta^o\boldsymbol{R} = \begin{bmatrix} \Delta^o\boldsymbol{u}_1^{\,T} & -\Delta^o\boldsymbol{u}_1^{\,T}\,{}^o\boldsymbol{R}_1 \\ \Delta^o\boldsymbol{u}_2^{\,T} & -\Delta^o\boldsymbol{u}_2^{\,T}\,{}^o\boldsymbol{R}_2 \\ \vdots & \vdots \\ \Delta^o\boldsymbol{u}_6^{\,T} & -\Delta^o\boldsymbol{u}_6^{\,T}\,{}^o\boldsymbol{R}_6 \end{bmatrix}, \quad \Delta\boldsymbol{c}_{rvi} = \begin{bmatrix} \left[vec\left(\Delta^o\boldsymbol{u}_1\,{}^o\boldsymbol{r}_1^{\,T}\right)^T\right]^T \\ \left[vec\left(\Delta^o\boldsymbol{u}_2\,{}^o\boldsymbol{r}_2^{\,T}\right)^T\right]^T \\ \vdots \\ \left[vec\left(\Delta^o\boldsymbol{u}_6\,{}^o\boldsymbol{r}_6^{\,T}\right)^T\right]^T \end{bmatrix}. \qquad (15)$$

Therefore, Eqs.(13) and (15) are sensor equations which include principal errors.

Measurement Range		±20 [m/s²]
Resolution (at 60 Hz)		0.02 [m/s²]
Operating Voltage Range		3 ~ 5 [V]
Quiescent Supply Current		0.6 [mA]
Temp. Operating Range		0 ~ 70 [degree Celsius]
Size		5×5×2 [mm]
Gain error	$\lvert \Delta u_j \rvert / \lvert {}^j u_j \rvert$	±20 [%]
Absolute alignment error	$\lvert \Delta^j \alpha_j \rvert / \lvert {}^j u_j \rvert$, $\lvert \Delta^j \beta_j \rvert / \lvert {}^j u_j \rvert$	±1.75 [%]
Offset error	$\lvert \Delta a_{ofj} \rvert / g$	±200 [%]

Table 1. Specifications of the dual-axis accelerometer chip (Analog Devices, Inc. Accelerometer ADXL202E)

Error factor	$\Delta^o \boldsymbol{R}$			
Error definition	$\dfrac{\lvert \Delta^o \boldsymbol{u}_i \rvert_{\max}}{\lvert {}^o \boldsymbol{u}_i \rvert}$	$\dfrac{\lvert \Delta^o \boldsymbol{u}_i{}^T \, {}^o \boldsymbol{R}_i \rvert_{\max}}{\lvert {}^o \boldsymbol{u}_i{}^T \, {}^o \boldsymbol{R}_i \rvert}$	$\dfrac{\lvert {}^o \boldsymbol{u}_i{}^T \, \Delta^o \boldsymbol{R}_i \rvert_{\max}}{\lvert {}^o \boldsymbol{u}_i{}^T \, {}^o \boldsymbol{R}_i \rvert}$	$\dfrac{\lvert \Delta^o \boldsymbol{u}_i{}^T \, \Delta^o \boldsymbol{R}_i \rvert_{\max}}{\lvert {}^o \boldsymbol{u}_i{}^T \, {}^o \boldsymbol{R}_i \rvert}$
Estimated value	0.251	0.251	0.242×10^{-2}	0.651×10^{-3}

Error factor	$\Delta \boldsymbol{c}_{rvi}$		
Error definition	$\dfrac{\lvert vec\{(\Delta^o \boldsymbol{u}_i \, {}^o \boldsymbol{r}_i{}^T)^T\} \rvert_{\max}}{\lvert vec\{({}^o \boldsymbol{u}_i \, {}^o \boldsymbol{r}_i{}^T)^T\} \rvert}$	$\dfrac{\lvert vec\{({}^o \boldsymbol{u}_i \, \Delta^o \boldsymbol{r}_i{}^T)^T\} \rvert_{\max}}{\lvert vec\{({}^o \boldsymbol{u}_i \, {}^o \boldsymbol{r}_i{}^T)^T\} \rvert}$	$\dfrac{\lvert vec\{(\Delta^o \boldsymbol{u}_i \, \Delta^o \boldsymbol{r}_i{}^T)^T\} \rvert_{\max}}{\lvert vec\{({}^o \boldsymbol{u}_i \, {}^o \boldsymbol{r}_i{}^T)^T\} \rvert}$
Estimated value	0.251	0.247×10^{-2}	0.751×10^{-3}

Table 2. Estimated error values

4.2 Calibration method for sensor errors

In general, a sensor system is calibrated using a known reference input. In the proposed 6-DOF sensor, it is necessary to determine at least 42 ($6 \times 6 + 6$) components. However, in this system, as shown in Eqs.(13) and (15), the unknown errors constitute 24 components (i.e.,

$\Delta^o \boldsymbol{u} \in \boldsymbol{R}^{3\times 6}$ and $\Delta \boldsymbol{a}_{of} = \left[\Delta a_{of1} \;\; \Delta a_{of2} \cdots \Delta a_{of6}\right]^T \in \boldsymbol{R}^6$), and these components can be estimated by using only certain translational inputs (i.e., $\boldsymbol{\omega}_b = 0, \dot{\boldsymbol{\omega}}_b = 0$). Thus, Eq.(13) can be written as follows:

$$\boldsymbol{a}_m = \left({}^o\boldsymbol{R} + \Delta^o\boldsymbol{R}\right)\begin{bmatrix} {}^o\ddot{\boldsymbol{p}}_b + \boldsymbol{g} \\ 0 \end{bmatrix} + \Delta \boldsymbol{a}_{of}. \tag{16}$$

When the above equation is solved for $\Delta^o \boldsymbol{u}$ and $\Delta \boldsymbol{a}_{of}$, we obtain

$$\begin{bmatrix} {}^o\boldsymbol{A} & \boldsymbol{I}_{6\times 6} \end{bmatrix}\begin{bmatrix} \Delta^o \boldsymbol{u}_i \\ \Delta \boldsymbol{a}_{ofi} \end{bmatrix} = \boldsymbol{a}_m - {}^o\boldsymbol{U}\,{}^o\ddot{\boldsymbol{p}}_{gb} \;,$$

$$\begin{aligned} {}^o\boldsymbol{A} &= \begin{bmatrix} {}^o\ddot{\boldsymbol{p}}_{gb}{}^T & & \\ & \ddots & \\ & & {}^o\ddot{\boldsymbol{p}}_{gb}{}^T \end{bmatrix}, \; {}^o\ddot{\boldsymbol{p}}_{gb} = {}^o\ddot{\boldsymbol{p}}_b + \boldsymbol{g} \;, \\ \Delta^o \boldsymbol{u} &= \left[\Delta^o \boldsymbol{u}_1{}^T \cdots \Delta^o \boldsymbol{u}_6{}^T\right]^T \;, \; {}^o\boldsymbol{U} = \left[{}^o\boldsymbol{u}_1{}^T \cdots {}^o\boldsymbol{u}_6{}^T\right]^T. \end{aligned} \tag{17}$$

In case Eq.(17) is measured *n* times,

$${}^o\boldsymbol{B}_n \begin{bmatrix} \Delta^o \boldsymbol{u} \\ \Delta \boldsymbol{a}_{of} \end{bmatrix} = \begin{bmatrix} \boldsymbol{a}_m - {}^o\boldsymbol{U}\,{}^o\ddot{\boldsymbol{p}}_{gb1} \\ \boldsymbol{a}_m - {}^o\boldsymbol{U}\,{}^o\ddot{\boldsymbol{p}}_{gb2} \\ \vdots \\ \boldsymbol{a}_m - {}^o\boldsymbol{U}\,{}^o\ddot{\boldsymbol{p}}_{gbn} \end{bmatrix}, {}^o\boldsymbol{B}_n = \begin{bmatrix} \begin{bmatrix} {}^o\boldsymbol{A}_1 & \boldsymbol{I}_{6\times 6} \end{bmatrix} \\ \begin{bmatrix} {}^o\boldsymbol{A}_2 & \boldsymbol{I}_{6\times 6} \end{bmatrix} \\ \vdots \\ \begin{bmatrix} {}^o\boldsymbol{A}_n & \boldsymbol{I}_{6\times 6} \end{bmatrix} \end{bmatrix} \in \boldsymbol{R}^{6n\times 24}. \tag{18}$$

In Eq.(18), ${}^o\boldsymbol{B}_n$ becomes a square matrix when *n*=4, whose number is the least number of measurement times, i.e., the principal errors $[\Delta^o \boldsymbol{u}^T \;\; \Delta \boldsymbol{a}_{of}{}^T]^T$ can be estimated using data for only four position.

4.3 A 6-DOF acceleration sensor system

A prototype of the 6-DOF accelerometer and the sensor specifications are shown in Fig.4 and Table 3, respectively. In this sensor, we used a dual-axis accelerometer ADXL202E (Analog Devices Co., Table 1), and installed microcomputer H8-3664 (Renesas Technology Co.) and a USB interface internally. This system captures signals from the accelerometers and transfers the data to the host computer at 60 Hz while performing integer arithmetic calculations in order to speed up the data processing.

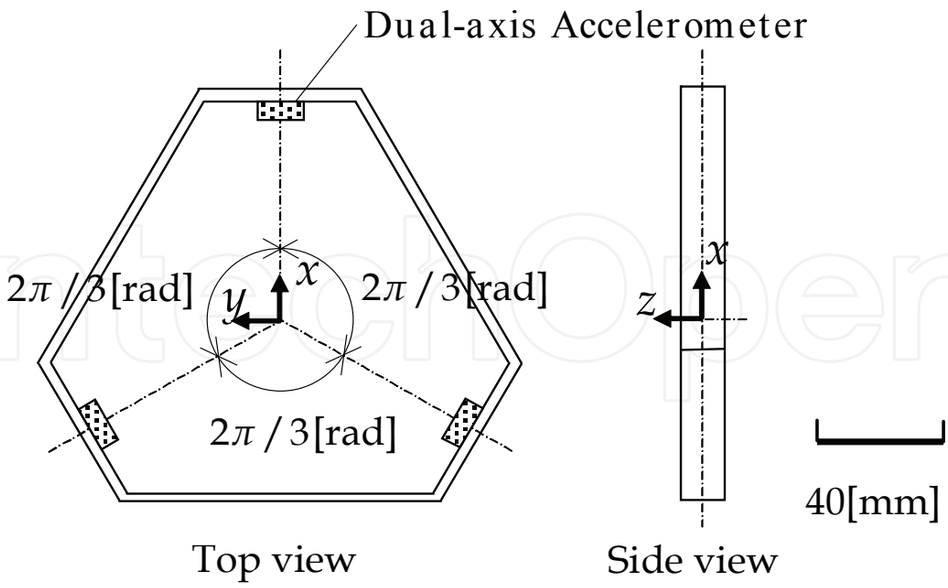

Fig. 4. Outline drawing of a prototype 6-DOF accelerometer

		Max	Typ	Resolution	Sampling
Translational	*x*	±19.6 [m/s²]	±9.8 [m/s²]	0.04 [m/s²]	60 [Hz]
	y				
	z				
Rotational	*x*	±490 [rad/s²]	±163 [rad/s²]	0.64 [rad/s²]	
	y				
	z				

Table 3. Specifications of the prototype 6-DOF accelerometer

4.4 Calibration results

Figures 5 and 6 show the measurement results as compared with the state before and after the calibration. This result took the measurement value when the gravitational acceleration was added for an arbitrary direction in the *x*-*y* plane of the sensor. Then, the *z* axis of the 6-DOF sensor was fixed in horizontally direction, and we rotated the sensor in the yaw direction. In addition, the difference between the values before and after the calibration was divided by the rated value (1G), and was thus represented as a dimensionless parameter. In Fig.5, the gain and offset error rates were reduced to 1% or less from about 2% and 4%, respectively. Then, the result from measuring the values along the *x* axis and the roll acceleration are shown in Fig.6. These accelerations should become essentially zero; however, the measurement values were perturbed by the offset error and the interference with the *y* axis the before calibration. After the calibration, the offset errors and the interference were reduced, and thus the availability of this calibration method was demonstrated.

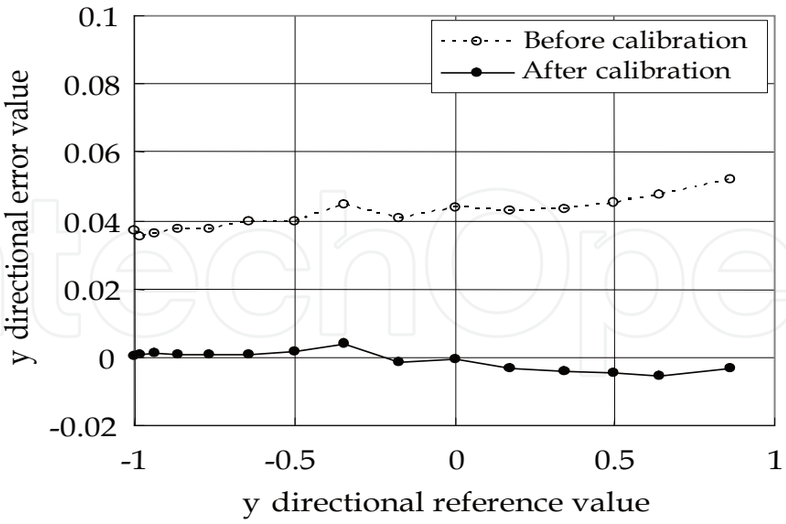

Fig. 5. *y* directional error characteristic before and after the calibration

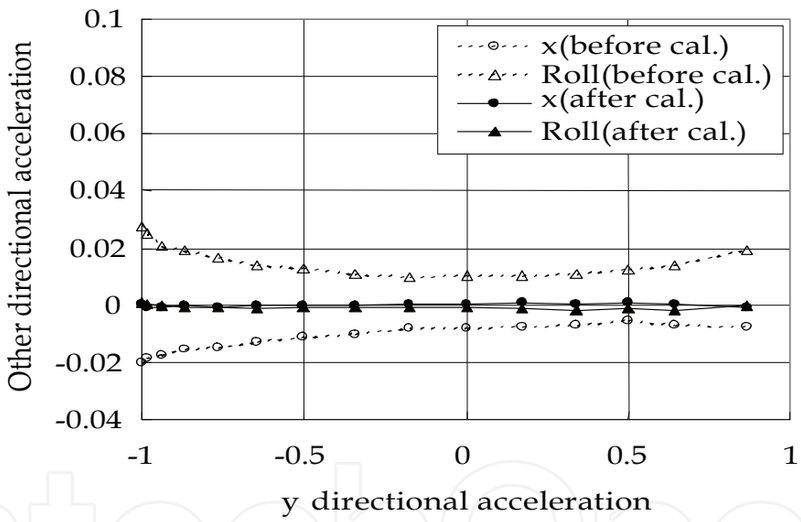

Fig. 6. Interference of the y directional acceleration to the other directions

5. Application to vehicle motion

5.1 Experimental task

In this section, we install the prototype sensor (see Table 3 and Fig.4) in a vehicle and investigate the applicability of the proposed methods to a relatively complex motion. The experimental task is the double lane change that involves the vehicle changing lane twice for a distance of about 2.5 m on a straight track. This task is known that detection of rotational components is relatively difficult because the influence of translational motion is large. Additionally, translational components are likely to become mixed with rotational components, which in turn is likely to induce the cross effect.

5.2 Experimental results

The experimental results are shown in Fig.7. In this experiment, we used a highly accurate triaxial rate sensor (Tamagawa Seiki Co.) which is unaffected by lateral motion as a reference. In the results, angular acceleration was transformed into angular velocity by numerical integration for the purpose of comparison with the rate sensor outputs. In addition, we applied a high-pass filter in order to suppress the drift error from emerging after integration. Figure 7 shows a comparison of the experimental results before and after the calibration in order to demonstrate the applicability of the above calibration method. Before performing the calibration, a large angular velocity was measured in the pitch direction, which should be almost zero, since the lateral components interfered with the rotational component. On the other hand, after performing the calibration, the cross effect was greatly reduced while at the same time the gain and the offset error were suppressed, and therefore the angular velocities were in good agreement with the rate sensor outputs. As a result, the applicability of this sensor system to a relatively complex motion was demonstrated.

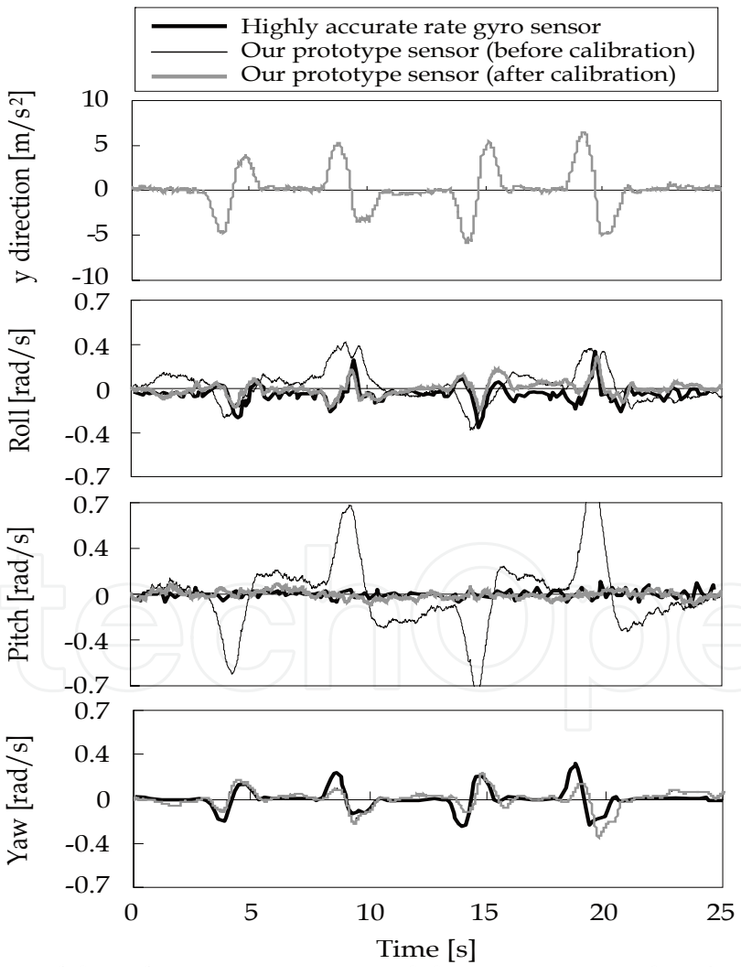

Fig. 7. Comparison of the reference gyroscope and the prototype acceleration sensor in double lane change experiment

6. Conclusion

This chapter described the stability and the error analysis of the proposed 6-DOF motion sensor system. A summary of the results is provided below.

1. This sensor system using multiple linear accelerometers can perform 6-DOF acceleration measurements by resolving each linear accelerometer outputs and CF terms, in other words, the terms consisting of angular velocities (see Eq.(8)). In order to clarify the instability conditions for this system, we analyzed the differential equation for the error by taking the measurement errors into account. As a result of analyzing the geometric instability conditions, the measurement errors increase rapidly when the roll or pitch frequency become even for the yaw motion and thus becomes unstable. However, it is unlikely for the system to become unstable under the influence of the above conditions in a rigid body motion, such as the motion of a vehicle or anaircraft.
2. The alignment errors of this sensor system consist of the position $(\Delta^o \boldsymbol{r}_i)$, sensitivity $(\Delta^o \boldsymbol{u}_i)$, and offset errors $(\Delta \boldsymbol{a}_{of})$. However, in this system, the principal errors are the offset and sensitivity errors since $\Delta^o \boldsymbol{r}_i$ is negligibly small (see Table 2). Thus, these errors can be estimated by using only four linear inputs (acceleration of gravity), and can be calibrated with relative ease and high accuracy for all 6 DOF.
3. We performed an experiment invoving a vehicle changing lanes twice (a double lane change task) using the prototype sensor, and the results demonstrated the applicability of the proposed system to relatively complex motion (see Fig.7).

7. References

Fraden, J. (2003). *Handbook of Modern Sensors*, AIP Press, page numbers (301-322), ISBN 0387007504

Padgaonkar,A.J, Krieger, K.W & King,A.I. (1975). Measurement of Angular Acceleration of a Rigid Body Using Linear Accelerometers. *Transaction of the ASME Journal of Applied Mechanics*, 42, page numbers (552-556)

K. Ohta, K. Kobayashi. (1994). Measurement of Angular Velocity and Angular Acceleration in Sports Using Accelerometers. *Transactions of the Society of Instrument and Control Engineers*, Vol. 30, No. 12, (December and 1994) page numbers (1442-1448), ISSN 04534654

K. Ohta, K. Kobayashi. (1995). Measurement of Angular Velocity and Angular Acceleration in Sports Using Extended Kalman Filter. *Transactions of the Society of Instrument and Control Engineers*, Vol. 31, No. 9, (September and 1995) page numbers (1265-1272), ISSN 04534654

T. Masuda, Y. Tanizawa. (2001). Measurement Experiment of the 6 DOF Acceleration Using Multiple Sensors. *Research Report of Industrial Reasearch Division, Mie Pref. Science & Techonology Promotion Center*, No.26, page numbers (117-120), ISSN 13478796

N. Mimura, R. Onodera. (2005). Stability Analysis of 6 DOF Acceleration Sensor System Using Multiple Accelerometers. *Transactions of the Japan Society of Mechanical Engineers Series C*, Vol. 71, No. 707, (July and 2005) page numbers (2218-2224), ISSN 03875024

N. Mimura, R. Onodera. (2006). Calibration Method for 6 DOF Acceleration Sensor Systems Using Multiple Accelerometers. *Transactions of the Japan Society of Mechanical Engineers Series C*, Vol. 72, No. 724, (December and 2006) page numbers (3798-3805), ISSN 03875024

R. Onodera, N. Mimura. (2006). A Stability of Six-Degrees-of-Freedom Acceleration Sensor System by Integration of Acceleration Signals (Considerations about a Dynamic Influence of Centrifugal Force Term in the Multi-Degree-of-Freedom Motion). *Transactions of the Japan Society of Mechanical Engineers Series C*, Vol. 72, No. 724, (December and 2006) page numbers (3789-3797), ISSN 03875024

R. Onodera, N. Mimura. (2008). Measurement of a Vehicle Motion Using a New 6-DOF Motion Sensor System –Angular Velocity Estimation with Kalman Filter Using Motion Characteristic of a Vehicle-. Journal of Robotics and Mechatronics, Vol.20, No.1, (February and 2008) page numbers (116-124), ISSN 09153942

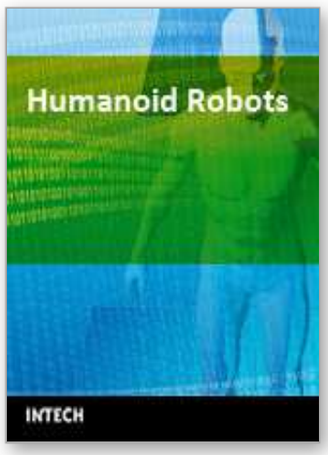

Humanoid Robots

Edited by Ben Choi

ISBN 978-953-7619-44-2
Hard cover, 388 pages
Publisher InTech
Published online 01, January, 2009
Published in print edition January, 2009

Humanoid robots are developed to use the infrastructures designed for humans, to ease the interactions with humans, and to help the integrations into human societies. The developments of humanoid robots proceed from building individual robots to establishing societies of robots working alongside with humans. This book addresses the problems of constructing a humanoid body and mind from generating walk patterns and balance maintenance to encoding and specifying humanoid motions and the control of eye and head movements for focusing attention on moving objects. It provides methods for learning motor skills and for language acquisition and describes how to generate facial movements for expressing various emotions and provides methods for decision making and planning. This book discusses the leading researches and challenges in building humanoid robots in order to prepare for the near future when human societies will be advanced by using humanoid robots.

How to reference

In order to correctly reference this scholarly work, feel free to copy and paste the following:

Ryoji Onodera and Nobuharu Mimura (2009). 6-DOF Motion Sensor System Using Multiple Linear Accelerometers, Humanoid Robots, Ben Choi (Ed.), ISBN: 978-953-7619-44-2, InTech, Available from: http://www.intechopen.com/books/humanoid_robots/6-dof_motion_sensor_system_using_multiple_linear_accelerometers

INTECH
open science | open minds

InTech Europe
University Campus STeP Ri
Slavka Krautzeka 83/A
51000 Rijeka, Croatia
Phone: +385 (51) 770 447
Fax: +385 (51) 686 166
www.intechopen.com

InTech China
Unit 405, Office Block, Hotel Equatorial Shanghai
No.65, Yan An Road (West), Shanghai, 200040, China
中国上海市延安西路65号上海国际贵都大饭店办公楼405单元
Phone: +86-21-62489820
Fax: +86-21-62489821

IntechOpen